

Effect of topology on dynamics of knots in polymers under tension

R. MATTHEWS, A.A. LOUIS and J.M. YEOMANS

¹ *Rudolf Peierls Centre for Theoretical Physics, 1 Keble Road, Oxford OX1 3NP, England*

PACS 02.10.Kn – Knot theory

PACS 87.15.-v – Biomolecules

PACS 82.35.Lr – Physical properties of polymers

Abstract. - We use computer simulations to compare the dynamical behaviour of torus and even-twist knots in polymers under tension. The knots diffuse through a mechanism similar to reptation. Their friction coefficients grow linearly with average knot length for both knot types. For similar complexity, however, the torus knots diffuse faster than the even twist knots. The knot-length auto-correlation function exhibits a slow relaxation time that can be linked to a breathing mode. Its timescale depends on knot type and exhibits a large jump between the most simple (3_1 and 4_1) knots and the more complex topologies. These differences in dynamical behaviour are interpreted in terms of topological features of the knots.

The scientific study of knots has a long history, dating back at least to the investigations of Johann Friedrich Gauss in the early 19th century. More recently, deep connections between knot theory, statistical mechanics [1] and quantum field theory [2] have stimulated a great deal of research both in physics and mathematics.

The discovery of knots in bacterial DNA [3] and in proteins [4–6], as well as earlier work on synthetic polymers [7] helped broaden the relevance of knot theory to the domain of chemistry and biology. Indeed, knots and links can be introduced *in vivo* into cellular DNA through processes such as replication [8] and are regulated through enzymes such as type II topoisomerases that can both knot and unknot DNA [9]. Biologists have exploited these topological effects to make many discoveries about the nature of DNA inside cells [10]. DNA is thought to be highly knotted inside some viral capsids [11], and we have recently suggested that these knots may control the ejection speed of a bacteriophage’s DNA into its host [12].

The discovery of knots in nature raises further questions about the dynamic properties of knotted polymers. In contrast to unknotted polymers, where dynamic behaviour is fairly well understood [13], many basic questions remain open. In polymers without tension, a long topological time-scale, not predicted by the standard Rouse model for polymer dynamics [13], was first discovered in the relaxation dynamics of the radius of gyration for knotted polymers [14]. Later work showed that this topological relaxation time decreased with increasing knot complex-

ity [15], and could also be observed by measuring the knot length autocorrelation function [16]. Related work [17, 18] showed that, by contrast, this time-scale increased with knot complexity when knotted ring polymers are cut.

Knots can be artificially introduced into biopolymers such as actin filaments [19] and linear DNA [20] with single molecule techniques. The Quake group [20] measured the diffusion coefficients of DNA knots by fluorescence microscopy. The knot friction coefficient grew roughly linearly with knot length, so that more complex knots diffused more slowly. Similar diffusion coefficients were obtained by the computer simulations of Vologodskii [21].

The experiments performed in ref. [20] utilized tensions ranging between 0.1-2 pN , which may be in a similar range to forces induced *in vivo* by enzymes such as polymerases [22]. Huang and Makarov [23] showed that the experiments were in the intermediate tension “elastic” regime where the external force $f > k_B T / l_p$, with l_p the persistence length of the polymer. Here the force aligns the segments of the chain in the general direction of the force, and the knot size is determined by the bending elasticity of the chain vs the force. The diffusion coefficient is only weakly dependent on tension, an effect also observed in experiments [20]. The elastic regime is bounded from above by a “tight knot” regime where $f \gg k_B T / l_p$ and the knot properties are dominated by details of the molecular interactions between monomers. By contrast, at the much lower tensions $f \ll k_B T / l_p$ of the “blob” regime, the knot size fluctuates widely.

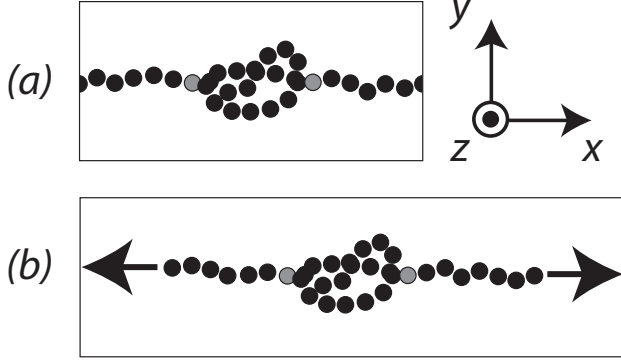


Fig. 1: The two geometries used in the simulations. In (a) the polymer ends are connected using periodic boundary conditions, forming a ring polymer under tension. In (b), the polymer is linear and the two end beads are subjected to a constant force to provide the tension. Grey circles indicate the beads identified as the first and last beads of the knot by the knot tracking algorithm

Most of the previous work on the dynamics of knots has focussed on the “blob” regime. However experiments on artificially knotted DNA [20], as well as the expectation that some knots *in vivo* may be held under tension [12,22], means that it is important to explore the effect of topology on knot dynamics in the elastic regime. This task will be the main focus of the present paper.

In this study we focus on two classes of knot topologies: torus knots and even-twist knots. The first few knots in each group are shown in Fig. 2 from which it is clear that knots of higher complexity have more crossings but a similar structure. We use the standard notation C_k where C denotes the minimal number of crossings in a projection of the knot onto a plane, and k is an index that distinguishes between knots with the same number of crossings [24].

To study the behaviour of knots in polymers under tension we used a bead-spring model coupled to a coarse grained solvent [12, 25, 26] that we briefly describe here. The polymer beads interact via the potential:

$$\beta V = 4\beta\epsilon \sum_{j>i} \sum_i \left[\frac{\sigma}{|\vec{r}_i - \vec{r}_j|} \right]^{12} - \frac{kR_0^2}{2} \sum_i \ln \left[1 - \left(\frac{|\vec{r}_i - \vec{r}_{i-1}|}{R_0} \right)^2 \right] \quad (1)$$

where the first term is an excluded volume interaction between beads and the second term is a FENE spring potential to simulate the bonds. The parameters were chosen as: $\beta\epsilon = 1$, $\sigma = 1$, $k = 30$ and $R_0 = 1.5$. The equations of motion of the beads were integrated with a velocity Verlet molecular dynamics algorithm.

In addition, the polymer was coupled to a mesoscopic solvent modelled with stochastic rotation dynamics (SRD) [27]. On average there are 5 solvent particles

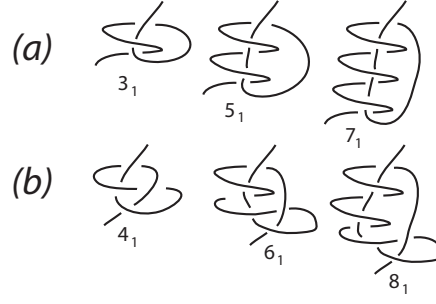


Fig. 2: (a) The first three torus knots. (b) The first three even-twist knots.

per volume σ^3 , and they provide a thermostat which conserves momentum and so preserves hydrodynamic interactions (HI) between monomers. The model thus describes a flexible polymer undergoing Brownian motion in a hydrodynamic solvent [25, 26].

To simulate a polymer under tension, two different geometries, illustrated in fig. 1, were considered. In the geometry (a), a simulation box of 32σ by 32σ by approximately 20σ was used. The polymer was connected to itself across the periodic boundary.

By varying the number of beads in the polymer, the tension can be changed. This approach offers the advantage that there are no free ends. Simulations may be run for as long as necessary to get good statistics without worrying about the knot coming undone or other end effects. In the geometry (b), a much larger simulation box of 32σ by 32σ by 300σ was used and the polymer ends were not joined. Instead the first and last beads were subjected to a constant force to provide tension. Geometry (b) was mainly used to test the reliability of the more efficient geometry (a).

Knots were introduced by hand. The first and last beads of a knot, shown in fig. 1, can be identified by finding bond crossings of bead to bead vectors from the projection of the polymer in a plane perpendicular to the tension force (x-y plane in fig. 1). The midpoint between the first and last beads was taken as the knot’s position and the difference as its length. Distances were measured along the polymer contour, as in the DNA experiments [20].

Fig. 3 shows that the length of the 3_1 knot decreases with tension and plateaus at higher tension, consistent with ref [23]. This behaviour holds for other knots as well. We will primarily use a tension of $f = 5 \frac{k_B T}{\sigma}$, putting us in the elastic regime since for a flexible polymer $\sigma \sim l_p$. If we were modeling DNA, where $l_p \approx 50nm$, our force would map onto $f \approx 0.4$ pN, which is comparable to the experiments of Bao *et al.* [20] who used forces in the range of 0.1 to 2 pN, placing them also in the elastic regime.

In table 1 we compare the average length of different knots for polymers under a tension of $f = 5 \frac{k_B T}{\sigma}$. The knot length increases approximately linearly with the number of essential crossings, an effect we observe at other tensions as well. For geometry (a) it is harder to set the

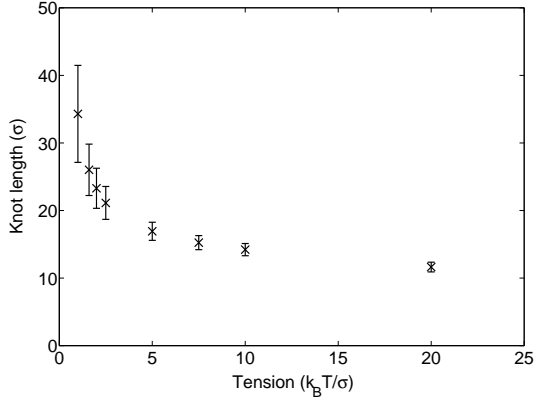


Fig. 3: Average knot length for the 3_1 knot on a polymer under tension. Simulations are done with geometry (b).

tension explicitly. Instead either the number of polymer beads was changed, or the box length was varied between $L = 20\sigma$ and $L = 21\sigma$ (the SRD algorithm uses boxes of size σ and so constrains the length to integer values). By comparing the knot length to the linear geometry, a similar effective tension could be simulated. We tested that the knot diffusion coefficient only depends very weakly on tension in the range $f = 2 - 8 \frac{k_B T}{\sigma}$, as expected for the elastic regime [20, 23].

We begin by studying the diffusive motion of the knots along the chain. In Fig. 4 we show the mean square displacement of the torus and even-twist knots as a function of time, measured in simulation units $t_0 = (\sigma/2)\sqrt{m_f/k_B T}$, where m_f is the mass of a fluid particle. At shorter times, we observe sub-diffusive behaviour with $\langle x^2 \rangle \sim \sqrt{t}$, but this crosses over to Fickian diffusive motion at later time scales, typically around $t \gtrsim 10^5 t_0$. The resulting diffusion coefficients, extracted from the mean-square displacements at later times (typically $t = 10^5 - 2 \times 10^5 t_0$), are listed in table 2. The diffusion coefficients clearly decrease with increasing crossing number, but for a given complexity, the torus knots have larger diffusion coefficients than the even-twist knots. We observed a similar topology induced non-monotonic behaviour with crossing number in simulations of knotted polymer ejection from a virus-capsid [12].

The diffusion coefficient can be related to the friction coefficient through the Einstein relation $\xi = k_B T / D$, and we show the results for friction vs. knot length in Fig. 5. Both types of knot show the same linear dependence on length, with the same slope, but there is a constant shift between them. A very similar linear dependence of the friction on length was measured in experiments [20] as well as in simulations [23]. In both cases the only even-twist knot measured was the 4_1 knot, and the friction was consistently higher than that expected from torus knots of the same length. We also plot a simple approximation to the friction, $\zeta \times$ the average knot length, where ζ is

Table 1: Average knot length for linear polymers under a tension of $5 \frac{k_B T}{\sigma}$ for geometries (a) and (b).

Knot type	Length in (b) geometry(σ)	Length in (a) geometry(σ)
3_1	17 ± 1	17 ± 1
4_1	24 ± 2	24 ± 1
5_1	28 ± 2	29 ± 2
6_1	35 ± 2	35 ± 2
7_1	39 ± 2	39 ± 2
8_1	46 ± 3	45 ± 2
9_1	49 ± 3	50 ± 2
10_1	56 ± 3	57 ± 2
11_1	59 ± 3	59 ± 2
12_1	66 ± 3	67 ± 2

the friction coefficient of a monomer in the SRD solvent. This simple approximation provides a good estimate of the slope of the friction vs. knot length curve in this tension regime, as also seen in ref. [23].

For unknotted polymers, neglecting the HI (Rouse approximation) leads to a linear dependence on the number of beads, but taking the hydrodynamics into account (Zimm approximation) changes the scaling substantially [13]. The methods used in refs. [21, 23] neglect HI, but the simulation technique we use here can reproduce the correct Zimm scaling for linear polymers [25, 26]. Including HI interactions *quantitatively* changes the magnitude of the knot diffusion coefficients by about a factor of 1.5 but does not appear to alter their *qualitative* scaling with knot length.

The difference in friction between torus and even-twist knots can be linked to an important topological distinction between them. As the knots diffuse along the chain, they must reptate through themselves [20]. From fig. 2, one can appreciate that the polymer may pass relatively smoothly through a torus knot, always curving in the same sense. For an even-twist knot, however, the twist at one end introduces a sharp inversion of the direction in which the polymer is curving, making the polymer passage through the knot less smooth and increasing the effective friction. Since this inversion occurs only once in an even-twist knot, it may explain why the frictions are higher than those of the torus knots by an additive constant.

Evidence that the main mode of knot diffusion in this regime is through reptation can be found in the mean-square displacement data in Fig. 4. At short times the motion is sub-diffusive because as the polymer in the knot tries to move it tends to be bounced back by other sections of the knot. At longer times, when the polymer contour has relaxed within the constraints formed by the knot, we observe ordinary Fickian diffusion. This crossover corresponds to two regimes in the reptation model [13] where the mean squared displacement of the polymer *along its own contour* increases with the exponents we observe.

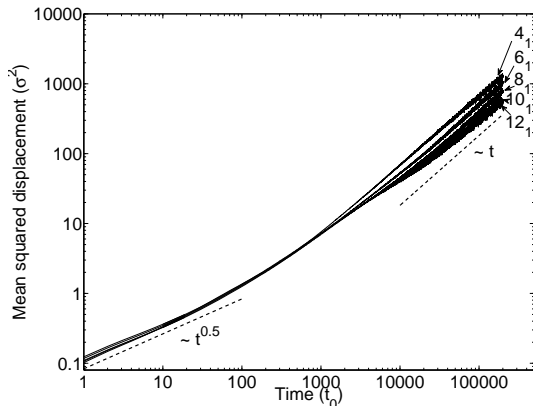


Fig. 4: Mean squared displacement curves plotted on log-log scales. The upper graph shows the torus knots, the lower the even-twist knots. The dashed lines have slopes of 0.5 and 1.

The mapping of dynamics from coarse-grained simulation units to physical units is always subtle [28]. In the experiments of ref. [20], $D \approx 1.25 \mu\text{m}^2/\text{s}$ for a 3_1 knot. Comparing to our simulated value for the same knot, and assuming $l_p \sim \sigma$ gives a mapping of $t_0 \approx 16 \mu\text{sec}$. Very similar values for t_0 are found when using the other knots to do the mapping. This suggests that sub-diffusive $\langle x^2 \rangle \sim \sqrt{t}$ behaviour should persist up to a time-scales of order ms , with the full crossover to Fickian diffusion occurring at time scales on the order of s . These time-scales should be accessible to experiments.

We next investigate the fluctuations and dynamic modes of the diffusing polymer knot under tension. Orlandini *et al* [16] showed that the long timescale originally observed in the radius of gyration autocorrelation function in the “blob” regime [14] can also be observed in the decay of the knot length autocorrelation function $\frac{\langle l(t)l(0) \rangle - \langle l(0) \rangle^2}{\langle l(0)l(0) \rangle - \langle l(0) \rangle^2}$, where $l(t)$ is the length of the knot at a given time. We investigated the same autocorrelation function for knots under tension, and plot the results in Fig. 6. The decay of the knot length autocorrelation function is approximately exponential, and the associated timescale (the inverse of the slope of the lines) of this exponential decay depends on the knot type, see table 2. The timescale increases with knot complexity and it is also significantly longer for torus knots than for even-twist knots of similar complexity. Moreover, there is a remarkably large jump (a factor of about 100) in the decay timescale between the most simple knots (3_1 and 4_1) and the more complex knots (5_1 and larger):

To identify the source of the slow decay of the knot length autocorrelation function, the configurations adopted by the knots were more closely investigated. Two different modes were identified: a spiral-flipping mode and a breathing mode, both depicted in fig. 7(a).

The spiral-flipping mode involves the knot switching between a state where the strand entering from the left pre-

Table 2: Relaxation time-scales and diffusion coefficients for knots in a polymer under tension.

Knot type	Relaxation time-scale ($\times 10^3 t_0$)	Diffusion coefficient ($\times 10^{-3} \frac{\sigma^2}{t_0}$)
3_1	0.020 ± 0.001	8.0 ± 0.4
4_1	0.029 ± 0.001	3.1 ± 0.2
5_1	2.1 ± 0.1	4.5 ± 0.3
6_1	1.2 ± 0.1	2.5 ± 0.2
7_1	2.5 ± 0.1	3.4 ± 0.2
8_1	1.4 ± 0.1	2.0 ± 0.1
9_1	3.5 ± 0.1	2.3 ± 0.2
10_1	1.9 ± 0.1	1.4 ± 0.1
11_1	5.2 ± 0.1	2.1 ± 0.1
12_1	2.1 ± 0.1	1.3 ± 0.1

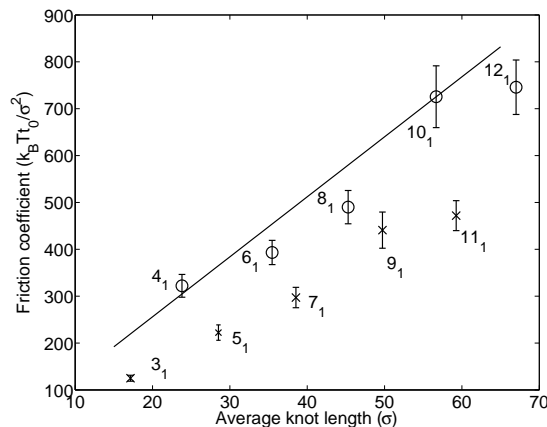


Fig. 5: Friction coefficient against average knot length for torus knots (crosses) and even-twist knots (circles). The solid line is $\zeta \times$ average knot length, where ζ is the friction coefficient of a monomer in the SRD solvent (each bead contributes a length of σ to the knot.)

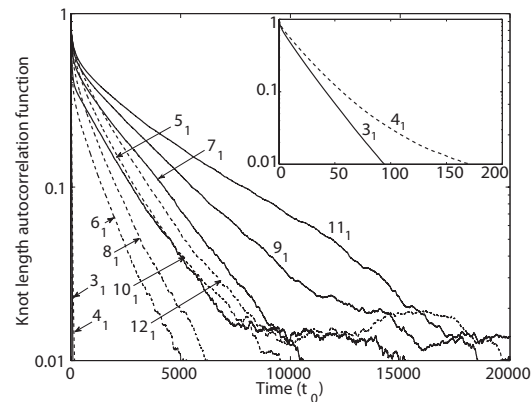


Fig. 6: Decay of the knot length autocorrelation with time. Results for torus knots are plotted using solid lines and for even-twist knots using dashed lines. The inset shows 3_1 and 4_1 results on a different scale.

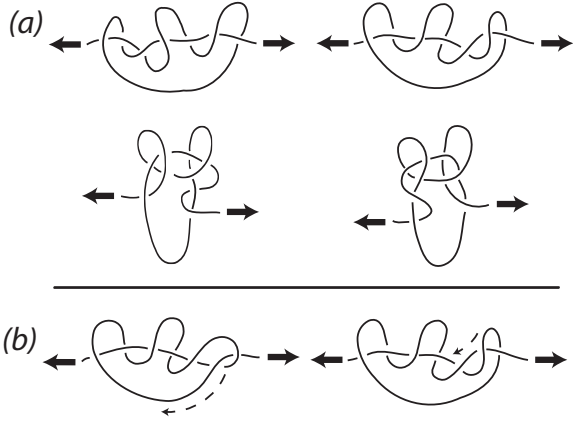


Fig. 7: (a) Examples of different knot states (for the 7_1 knot). The arrows indicate the direction of the tension force. The change between the left and right configurations involves inverting the spiral - the spiral-flipping mode. The change between the upper and lower configurations involves switching the alignment of the spiral with respect to the tension force - the breathing mode. (b) Origin of the faster breathing mode seen in the even-twist knots. Left: in even twist knots, the end of the spiral, the twist, may slide relatively freely along the strand that passes through it. Right: if the end of the spiral moves in a similar manner in a torus knot it will collide with the other loops of the spiral.

dominantly curves around the strand entering from the right and vice-versa. The breathing mode involves the knot switching between a state where the axis of the spiral is aligned with the tension force and one where the spiral forms a loop perpendicular to the tension force. To characterise the state of the knot, two order parameters were used: one to capture the spiral-flipping mode and another for the breathing mode.

For the spiral-flipping mode the sum of angles between successive bonds - in the plane defined by those bonds - multiplied by the displacement from the centre of the knot was taken over all of the beads in the knot. Depending on whether the polymer is more curved towards one end of the knot or the other, this quantity will take positive or negative values. For the breathing mode the ratio between the maximum distance between any two beads in the knot in the direction of the tension force to the maximum distance perpendicular to the tension force was taken. When the spiral of the knot is aligned with the tension this quantity will have a higher value.

We calculated the autocorrelation functions, $\frac{\langle \phi(t)\phi(0) \rangle - \langle \phi(0) \rangle^2}{\langle \phi(0)^2 \rangle - \langle \phi(0) \rangle^2}$, where ϕ is the value of the order parameter, for these two order parameters. As an example, the autocorrelation functions for the 3_1 and 11_1 knots are depicted in fig. 8. The breathing autocorrelation function has a very similar decay to the knot length autocorrelation function, whereas the spiral flipping autocorrelation function decays more rapidly. Nevertheless, both modes show a large jump in time scale between the 3_1 and 4_1 and the more complex knots.

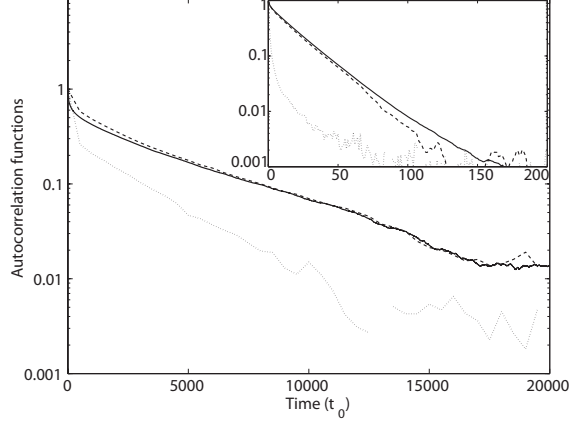


Fig. 8: Autocorrelation functions for 11_1 for the knot length (solid line), the breathing mode order parameter (dashed line) and the spiral-flipping mode order parameter (dotted line). The inset shows results for 3_1 on a different scale.

These results suggest that the breathing mode is responsible for the slow decay of the knot length autocorrelation. If the average knot lengths for high and low values of the breathing mode order parameter are calculated it is indeed seen that the extended configuration corresponds to a larger knot length; for the most complex knots a difference of about 3σ is observed.

The coupling to the breathing mode offers an explanation for the large jump in the timescale of the knot length autocorrelation decay between 3_1 and 4_1 and the more complex knots. The spiral of the most simple knots consists of only one loop and so shifting from a configuration which is extended in the direction of the tension only involves changing the shape of this one loop. In contrast, for the more complex knots, it involves the co-ordinated movement of multiple loops. It also offers an explanation for the difference between the torus and the even-twist knots. As depicted in fig. 7(b), an even-twist knot may deform from an extended configuration by sliding the twist along the strand that passes through it. In a torus knot the equivalent movement is blocked by the loops of the spiral, leading to a slower breathing mode.

Note that there is no big jump in the diffusion coefficients between the 3_1 and 4_1 topologies and the more complex knots. While the breathing and spiral-flipping modes may affect the crossover from sub-diffusive to diffusive behaviour (in fact the sub-diffusive range is considerably shorter for the 3_1 and 4_1 knots) they do not appear to determine the long-time diffusive dynamics.

It is instructive to compare our results for the longest relaxation time-scale with those of previous work on ring polymers without tension. By contrast with our results, the long time-scale was shown to *decrease* with increasing knot complexity and no significant differences between knot groups was observed [15]. These differences suggest that the dominant modes that determine the relaxation in

the “blob” regime are not related to the breathing modes we observe for polymers under tension.

By contrast, simulations that studied the relaxation of initially knotted polymers that have been cut (without tension) [18] exhibited a relaxation time-scale that increased for increasing knot complexity, and that was longer for torus knots than for even-twist knots. The similarity is perhaps not surprising. For a cut knot to become unentangled the polymer must move along the contour formed by the erstwhile knot, a process analogous to the self-reptation [20] of knots under tension.

In summary: we exploited a new boundary condition that minimizes end-effects to study the effect of topology on the dynamics of knots in polymers under tension in the “elastic regime” where the force is strong enough to affect the behaviour of the knot, but not so strong that details of the inter-molecular potentials dominate the behaviour.

The observed motion of the knot, including a sub-diffusive regime of the mean-square displacement at short-times, is consistent with a self-reptation mechanism [20]. To first order, the friction coefficient scales linearly with the size of the knot. But topological differences also play a role. For a similar knot size or complexity, torus knots have a smaller friction (and so a larger diffusion coefficient) than even-twist knots.

The fluctuations and dynamic modes are also affected by the topology of the knot. The longest relaxation mode of the length-length autocorrelation function is dominated by a breathing mode. This topological timescale increases with knot complexity and is significantly longer for the torus knots than for even-twist knots of similar complexity. It shows a big jump between the two simplest (3_1 and 4_1) and the more complex knots. These differences can be rationalized by examining the topology of the different knots.

In this paper we have used a simple flexible polymer model. The main results summarized above should carry over to other polymer models. Nevertheless, it would be interesting, for example, to simulate semi-flexible polymers that provide a better model of DNA. In particular, this may give a more accurate estimate of the different physical time-scales, and aid experiments aimed at measuring them. In addition, it would be important to study the role of tension on DNA knots *in vivo* [22]. For example, what are the magnitudes of the biological forces, and what is the role of macromolecular crowding on knot diffusion and relaxation rates? Finally, the advent of nanotechnology has brought questions about the diffusion and dynamics modes of knotted polymers in strong confinement to the fore [29, 30]. It would be interesting to see how confinement affects the picture for knots under tension.

We thank Olivier Pierre-Louis and Enzo Orlandini for helpful discussions.

REFERENCES

- [1] JONES V., *Lect. Notes. Math.* , **1525** (1992) 70.
- [2] WITTEN E., *Commun. Math. Phys.* , **121** (1989) 351.
- [3] LIU L., DEPEW R. and WANG J., *J. Mol. Biol.* , **106** (1976) 439.
- [4] MANSFIELD M., *Nat. Struct. Biol.* , **1** (1994) 213.
- [5] KOLESOV G., VIRNAU P., KARDAR M. and MIRNY L. A., *Nucleic Acids Research* , **35** (2007) 425.
- [6] DZUBIELLA J., *Biophys. J.* , **96** (2009) 831.
- [7] FRISCH H. and WASSERMAN E., *Chemical Topology* , **83** (1961) 3789.
- [8] OLAVARIETTA L., MARTINEZ-ROBLES M. L., HERNANDEZ P., KRIMER D. B. and SCHVARTZMAN J. B., *Mol. Microbiol.* , **46** (2002) 699.
- [9] WATT P. M. and HICKSON I. D., *Biochem. J.* , **303** (1994) 681.
- [10] WASSERMAN S. and COZZARELLI N., *Science* , **232** (1986) 4753.
- [11] ARSUGA J., VAZQUEZ M., TRIGUEROS S., SUMNERS D. and ROCA J., *Proc. Nat. Acad. Sci. U.S.A.* , **99** (2002) 5373.
- [12] MATTHEWS R., LOUIS A. and YEOMANS J., *Phys. Rev. Lett.* , **102** (2009) 088101.
- [13] DOI M. and EDWARDS S., *The Theory of Polymer Dynamics* (OUP, Oxford) 1986.
- [14] QUAKE S. R., *Phys. Rev. Lett.* , **73** (1994) 3317.
- [15] LAI P.-Y., *Phys. Rev E.* , **66** (2002) 021805.
- [16] ORLANDINI E., STELLA A. L., VANDERZANDE C. and ZONTA F., *J. Phys. A:Math. Theor.* , **41** (2008) 1.
- [17] SHENG Y.-J., LAI P.-Y. and TSAO H.-K., *Phys. Rev E.* , **58** (1998) 021805.
- [18] LAI P.-Y., SHENG Y.-J. and TSAO H.-K., *Phys. Rev. Lett.* , **87** (2001) 175503.
- [19] ARAI Y., YASUDA R., AKASHI K., HARADA Y., MIYATA H., JR K. K. and ITOH H., *Nature* , **399** (1999) 446.
- [20] BAO X. R., LEE H. J. and QUAKE S. R., *Phys. Rev. Lett.* , **91** (2003) 265506.
- [21] VOLOGODSKII A., *Biophys. J.* , **90** (2006) 1594.
- [22] LIU Z., DEIBLER R., SUN H. and ZECHIEDRICH L., *Nucleic Acids Res.* , **37** (2009) 661.
- [23] HUANG L. and MAKAROV D. E., *J. Phys. Chem.* , **111** (2007) 10338.
- [24] ORLANDINI E. and WHITTINGTON S. G., *Rev. Mod. Phys.* , **79** (2007) 611.
- [25] MALEVANETS A. and YEOMANS J., *Europhys. Lett.* , **52** (2000) 231.
- [26] RIPOLL M., MUSSAWISADE K., WINKLER R. and GOMMER G., *Europhys. Lett.* , **68** (2004) 106.
- [27] MALEVANETS A. and KAPRAL R., *J. Chem. Phys.* , **110** (1999) 8605.
- [28] PADDING J. and LOUIS A., *Phys. Rev. E.* , **74** (2006) 031402.
- [29] METZLER R., REISNER W., RIEHN R., AUSTIN R., TEGENFELDT J. O. and SOKOLOV I. M., *Europhys. Lett.* , **76** (2006) 696.
- [30] MOEBIUS W., FREY E. and GERLAND U., *Nano Lett.* , **8** (2008) 4518.